Human Molecular Genetics, 2010, Vol. 19, No. 8 ***1551–1560***
doi:10.1093/hmg/ddq028
Advance Access published on January 27, 2010

Defects in middle ear cavitation cause conductive hearing loss in the *Tcof1* mutant mouse

Carol A. Richter[1], Susan Amin[1], Jennifer Linden[2], Jill Dixon[3], Michael J. Dixon[3,4] and Abigail S. Tucker[1,*]

[1]Department of Craniofacial Development, Dental Institute, King's College London, London SE1 9RT, UK, [2]UCL Ear Institute, University College London, London, UK, [3]Faculty of Medical and Human Sciences, Manchester Academic Health Sciences Centre and [4]Faculty of Life Sciences, University of Manchester, Manchester, UK

Received December 11, 2009; Revised January 14, 2010; Accepted January 20, 2010

Conductive hearing loss (CHL) is one of the most common forms of human deafness. Despite this observation, a surprising gap in our understanding of the mechanisms underlying CHL remains, particularly with respect to the molecular mechanisms underlying middle ear development and disease. Treacher Collins syndrome (TCS) is an autosomal dominant disorder of facial development that results from mutations in the gene *TCOF1*. CHL is a common feature of TCS but the causes of the hearing defect have not been studied. In this study, we have utilized *Tcof1* mutant mice to dissect the developmental mechanisms underlying CHL. Our results demonstrate that effective cavitation of the middle ear is intimately linked to growth of the auditory bulla, the neural crest cell-derived structure that encapsulates all middle ear components, and that defects in these processes have a profoundly detrimental effect on hearing. This research provides important insights into a poorly characterized cause of human deafness, and provides the first mouse model for the study of middle ear cavity defects, while also being of direct relevance to a human genetic disorder.

INTRODUCTION

As one of the five human senses, hearing not only has critical biological function, but is also crucially important for our integration within society. Loss of hearing can cause severe impediment to normal social interaction and activities, has an impact on instinctive behaviors, and affects the normal development of speech and language skills. There are different forms of deafness, which are characterized according to the region of the ear apparatus that is affected. Disruptions to middle ear function result in conductive hearing loss (CHL), while defects in the inner ear result in sensorineural hearing loss. To date, most hearing research has concentrated on exploring the defects underlying sensorineural deafness. Consequently, a surprising gap in our understanding of the mechanisms underlying CHL exists, particularly with respect to the mechanisms underlying middle ear development and disease. Importantly many instances of conductive deafness (caused by the disruption of effective sound conduction through the external and/or middle ear apparatus via genetic disease, morphological anomaly or inflammation) can be alleviated through surgical or pharmaceutical intervention (1). In order to reduce patient suffering and improve treatment methodology, it is of critical importance that a fuller understanding of the underlying developmental processes is achieved.

Much of our current understanding of middle ear development has been elucidated through detailed otolaryngological study of dry skulls and analyses of murine embryogenesis (2–8). Such studies have revealed that formation of the mammalian middle ear structure is a highly intricate process that initiates in the second trimester in humans, mid-gestation in mice, starting with the early patterning of the middle ear bones (the malleus, incus and stapes). These bones form the ossicular chain along which sound vibrations are transmitted, across the middle ear space, from the outer ear to the inner ear (9). The middle ear ossicles are subsequently encased by the auditory bulla, a complex structure that forms from fusion of multiple intramembranous ossifications (6). This dynamic modeling of the middle ear apparatus takes place in

*To whom correspondence should be addressed at: Guy's Hospital, Floor 27, London SE1 9RT, UK. Tel: +44 2071887384; Fax: +44 2071881674; Email: abigail.tucker@kcl.ac.uk

conjunction with cavitation, the process through which the middle ear cavity is cleared of the mesenchymal tissue in which the middle ear ossicles initially develop (10–12). This process results in the production of an enclosed air space across which sound vibrations can be carried and it is therefore critical for effective hearing.

Cavitation is common to many animals (regardless of the number of middle ear ossicles in place) and proceeds mostly postnatally; however the precise mechanism(s) underlying mesenchymal 'clearing' have proved elusive. In the mouse, rat and human programmed cell death (apoptosis) has been shown to occur in the middle ear mesenchyme, starting prenatally and continuing throughout the cavitation process (12–14). The number of cells, however, are few and scattered throughout the mesenchyme. In addition apoptosis has not been observed during avian middle ear cavitation (10,13), indicating that this form of cell death may not play a central role. Large numbers of macrophages and phagocytes have been observed in the mesenchyme during cavitation in humans and chicks, which may act to remove degenerating mesenchymal cells (10,11). As an alternative theory, studies performed in developing human and opossum middle ears suggest that the mesenchyme does not disappear but is redistributed over the increasing surface area of the growing middle ear capsule (15,16). It seems likely that a combination of these mechanisms is occurring in the ear.

Incomplete removal of middle ear cavity mesenchyme, due to a failure in the cavitational process, has been shown to have severe clinical implications. In this context, failure of cavitation has been linked to the anomaly 'residual mesenchyme in adults' which has been identified as a contributory factor to otitis media in both children and adults (17), conditions that create a considerable healthcare burden (18). Various human syndromes present with cavitation defects (19,20). Treacher Collins Syndrome (TCS; OMIM 154500) is an autosomal dominant disorder of craniofacial development that results from loss-of-function mutations in the gene *TCOF1*; individuals affected by this disorder exhibit congenital CHL in over 50% of cases with middle ear defects observed in almost 100% of patients (21,22).

To date, the study of middle ear development has been hampered by the lack of mouse models with isolated middle ear anomalies (23); the majority of mouse mutants with perturbed middle ear development published exhibit either additional inner ear problems, which complicate analysis of the CHL, or exhibit such extreme craniofacial/developmental disruption that the developmental genetics of middle ear formation cannot be determined clearly. Thus identification of novel mouse models with defects restricted to the middle ear is therefore of great importance.

In this study, we have established that a loss-of-function mutation in *Tcof1* residing on a congenic DBA/1 genetic background results in defects in middle ear postnatal development and severe CHL. *Tcof1* is the mouse orthologue of the human *TCOF1* gene, mutations in which cause TCS (22,24,25). The *Tcof1* gene encodes the nucleolar phosphoprotein Treacle, which plays an important role in ribosome biogenesis (26). *Tcof1* exhibits a dynamic expression pattern, with high levels observed in the developing and migrating neural crest cells at embryonic day (E)8.5 and the neural crest-derived craniofacial tissues at E9.5 (27). The cranial mesoderm, in contrast, is negative for *Tcof1* expression. The levels of *Tcof1* reduce as the pharyngeal arches continue to form with expression largely undetectable by E12.5 (27). *Tcof1* mutant heterozygous ($Tcof1^{+/-}$) mice show an increase in apoptosis and reduced proliferation of cranial neural crest cells at early stages of initiation and migration, resulting in a reduced number of cranial neural crest cells populating the developing face. This deficit of crest cells is then responsible for the cranial hypoplasia of the facial skeleton that is characteristic of TCS in both humans and mouse models (27). In $Tcof1^{+/-}$ mice many of the defects observed phenocopy those exhibited by the human syndrome, although the severity of the phenotype is highly dependent on genetic background (28). Indeed, the more severe phenotypes result in embryonic or neonatal lethality, precluding analysis of anomalies associated with later development such as cavitation of the middle ear space. $Tcof1^{+/-}$ mice on a DBA/1 genetic background are, however, viable and we have identified that these mice have profound hearing problems and possess anomalies in middle ear cavitation and auditory bulla (AB) growth. The defects uncovered support the notion that mesenchymal clearance is linked to AB growth. We thus propose the *Tcof1/DBA1* mouse line as a murine model for cavitation defects and a means for the further study of the mechanisms at work during middle ear development.

Table 1. Preyer reflex analysis demonstrates that $Tcof1/DBA1^{+/-}$ mice exhibit defects in hearing

Genotype	Preyer reflex	
	Positive response	Negative response
WT	22	0
$Tcof1/DBA1^{+/-}$	5	14

A positive preyer response indicates that the animal produced a reflexive action due to an auditory stimulus (click); a negative response indicates the animal failed to do so.

RESULTS

Tcof1/DBA1 heterozygotes have significant hearing deficits

Potential middle ear defects in mice heterozygous for a loss-of-function allele on a DBA/1 genetic background have not been analyzed previously (28). Preyer reflex analysis revealed that in the majority of cases, Tcof1/DBA1 heterozygotes ($Tcof1/DBA1^{+/-}$) show defects in hearing, although some reflex was detected in ~30% of cases ($n = 5/19$) (Table 1). To identify more subtle phenotypes and to define hearing thresholds, a subset of mice were also examined using auditory brainstem response (ABR) (29). In keeping with the Preyer reflex analysis, mutant mice with no visible Preyer reflex showed no detectable ABR reading, indicating that these animals were completely deaf, while mice with a limited reflex showed a limited ABR response (Fig. 1A–C).

In TCS patients, deafness is associated with dysmorphic or missing ossicles and a hypoplastic middle ear cavity (21). To investigate whether similar defects contributed to the hearing

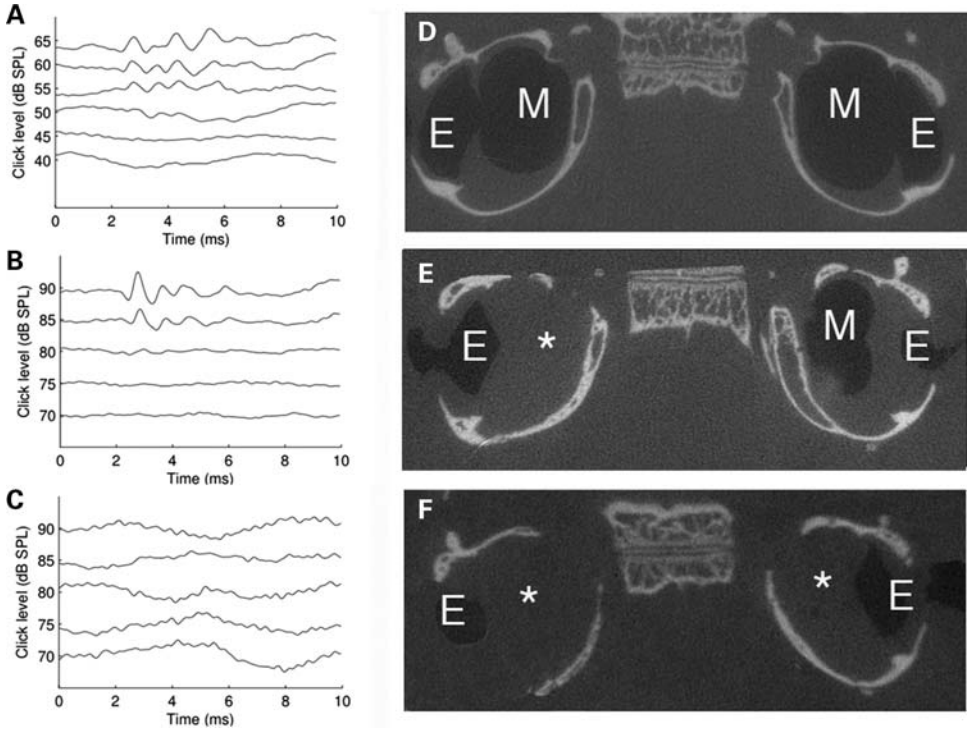

Figure 1. *Tcof1/DBA1*$^{+/-}$ mice exhibit partial or complete hearing loss. (**A**–**C**) Auditory brainstem response (ABR) measurements of wild-type and *Tcof1/DBA1*$^{+/-}$ mutant mice at 10 weeks. (A) Wild-type hearing threshold of 55 dB SPL; (B) *Tcof1/DBA1*$^{+/-}$ intermediary defect has a hearing threshold of 85 dB SPL; (C) *Tcof1/DBA1*$^{+/-}$ severe defect has no detectable hearing capacity. (**D**–**F**) Sections through microCT reconstructions of the same specimens as in (A–C). (D) Wild-type mouse. Air spaces (dark areas) are found in both the external (E) and middle ears (M). (E) *Tcof1/DBA1*$^{+/-}$ mouse. Air spaces are found in the external ears, but only in one of the middle ears. (F) *Tcof1/DBA1*$^{+/-}$ mouse. Air spaces are only observed in the external ears. Asterisk indicates regions lacking air spaces.

loss observed in *Tcof1/DBA1*$^{+/-}$ mice, we investigated ossicle development during embryonic and postnatal development and middle ear cavitation during postnatal development. Coincident with the CHL exhibited by human TCS patients, morphological analysis established that inner ear development was normal in *Tcof1/DBA1*$^{+/-}$ mice (data not shown). Similarly, skeletal analysis indicated that the middle ear ossicles formed at the correct stage and the joints between the ossicles were normal in *Tcof1/DBA1*$^{+/-}$ mice compared with their wild-type littermates (9) (Fig. 2A and B). MicroCT imaging in postnatal day (P)14 pups further revealed that the three-dimensional organization of the ossicular chain was identical in *Tcof1/DBA1*$^{+/-}$ mice and their wild-type littermates (Fig. 2C and D).

Tcof1/DBA1$^{+/-}$ mice have defects in cavitation of the middle ear space

Having found no defect in the development of the middle ear ossicles, we investigated formation of the middle ear cavity. Sections from microCT scans of the middle ear were analyzed in adult mice. In wild-type (WT) mice, the air-filled middle ear space was clearly visible in section as the air forms a black shadow within the middle ear; the external ear on the other side of the tympanic membrane was also filled with air and had a similar appearance (Fig. 1D). In a mouse that had shown no ABR response, a black air-filled space was visible in the region of the external ear, however a similar area was not found within the middle ear indicating the absence of an air-filled space (Fig. 1F). Of particular interest was the finding that in a mouse that showed a limited ABR response, a black region indicating an air-filled space was found in the middle ear on one side of the head but not on the other side indicating that this mouse had an asymmetric defect in middle ear cavity formation leading to partial hearing loss (Fig. 1E). A similar loss of middle ear air-filled spaces were observed by microCT in mice that showed no, or limited, Preyer's reflex (data not shown). To confirm the microCT findings, *Tcof1/DBA1*$^{+/-}$ mouse ears were analyzed histologically and found to contain large masses of mesenchyme filling the middle ear cavity and surrounding the ossicles (Fig. 3A). In contrast, WT littermates showed middle ears free from mesenchyme, with the ossicles suspended in an air-filled space (Fig. 3B). The mesenchymal tissue that is usually cleared from the middle ear to create an operational air-filled cavity was thus retained in the mutants. In keeping with the microCT results, the degree of mesenchyme retention varied between mice, but also varied within individuals between left and right ears (Table 2). All *Tcof1/DBA1*$^{+/-}$ mice showed some degree of mesenchymal retention, which correlated directly with their ability to hear (Table 2).

Little is known about how cavitation proceeds and so, to investigate this process, we analyzed middle ears from birth to completion of cavitation. Cavitation was most active from P6 onwards and is complete by P14 (Fig. 3B–F). Preyer reflex analysis at these stages confirmed the link between

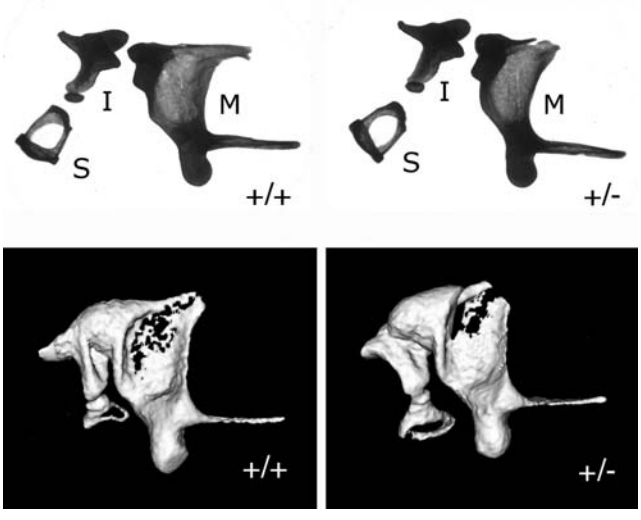

Figure 2. Normal ossicle development in *Tcof1*$^{+/-}$ mice on the DBA1 background. (**A** and **B**) Skeletal analysis of ossicles dissected apart at P21. No difference is observed in morphology of the three ossicle in (A) wild-type (+/+) and (B) mutant (+/−) mice. (**C** and **D**) MicroCT image of middle ear ossicles *in situ*. No difference is observed between the three ossicle in (C) wild-type (+/+) and (D) mutant (+/−_ mice). M, malleus; I, incus; S, stapes. Black gaps in the body of the malleus are due to the scan not detecting the thinner bone in this region.

cavitation and hearing; P6–P9 pups failed to respond to an auditory stimulus while P14 animals responded positively. The middle ears of P14 *Tcof1/DBA1*$^{+/-}$ mice appeared similar to those of WT mice at earlier developmental stages; consequently, to confirm that the retained mesenchyme was not due to a delay in cavitation, the middle ears of P49 *Tcof1/DBA1*$^{+/-}$ mice were also analyzed histologically. Retention of mesenchyme was clearly present in the mutant mice compared with their WT littermates (Supplementary Material, Fig. S1).

Defects in cavitation are linked with the size of the auditory bulla

From the microCT scans it was clear that, in addition to defects in the amount of air-filled space, the size of the auditory bulla that encapsulates the middle ear was reduced in *Tcof1/DBA1*$^{+/-}$ mice (Fig. 4A and B; Table 3). Auditory bulla formation proceeds postnatally in mice via intramembranous ossification. The mouse auditory bulla is a complex structure formed from fusion of a number of membranous skeletal elements, including the petrosal bone, retrotympanic process of the forming temporal bone, and tympanic ring (ectotympanic). These skeletal elements are distinct at birth (P0) and subsequently fuse to form the final bulla, which forms next to the cartilaginous otic capsule (*pars cochlearis*) (Fig. 5A–D). The bony template of the auditory bulla is laid down from P6, with the final pattern apparent by P9 (Fig. 5D). Analysis of middle ear cavity volume from microCT images (Table 3), implemented as a means of measuring auditory bulla growth, is consistent with previous analyses that used injection of alcohol to estimate the volume of the developing middle ear (30). These studies suggested the presence of a critical 'growth window' in AB development from P9 after which the auditory bulla increases in size radically up to P15, fulfilling most of its capacity by P21, with further, slight, expansion occurring later in adult life.

As *Tcof1* expression is associated earlier in development with neural crest cell-derived cranial tissues, we investigated the contribution of the neural crest to the auditory bulla and middle ear mesenchyme. A recent fate map using the *Mesp1*cre mouse to label cranial mesoderm marked some components of the auditory bulla as being of mesoderm origin at P0 (31). Given the potential defect in this structure in *Tcof1/DBA1*$^{+/-}$ mice, we re-investigated the origin of the auditory bulla using *Wnt1cre*/Rosa26 reporter mice. At P9, when the auditory bulla has developed into its distinctive shape, the whole of the auditory bulla that encapsulates the middle ear was shown to be neural crest-derived, while the originally cartilaginous, *pars cochlearis* over the inner ear remained negative, and is therefore presumably of mesoderm origin (Fig. 5E). In section the bulla is shown to stain strongly for lacZ, with the bony matrix picking up the pink counterstain (Fig. 5F). The mesenchyme that initially occupies the middle ear is also of neural crest origin and stains blue (Fig. 5G). The defect in the auditory bulla and middle ear mesenchyme is therefore in keeping with a defect in neural crest-derived tissues of the head.

Analysis of *Tcof1/DBA1*$^{+/-}$ mutant middle ear development (Table 3) revealed a significant reduction in middle ear cavity volume from P6, the earliest stage that volume of the auditory bulla can be measured by microCT. This size defect is maintained throughout later developmental stages. The phenotype is variable, however, with a 25% reduction in middle ear volume compared with WT being evident in the most severe cases. A reduction in the size of the auditory bulla was observed in both ears in some mice, while others showed an asymmetric loss with only one ear affected. Of particular significance was the finding that mesenchyme was retained in the ears with smaller auditory bullae, while ears with auditory bullae approaching WT size had successfully managed to clear the ears and create an air-filled space (Table 4, Figure 6); a correlation therefore exists between the size of the auditory bulla, the presence or absence of mesenchyme, and the ability to hear (Tables 3 and 4).

To investigate the underlying cause of the reduction in the size of the auditory bulla, proliferation and apoptosis studies were carried out. Previous research has shown that the defect in *Tcof1* mutant mice on genetic backgrounds that cause a more severe phenotype, is driven both by an increase in apoptosis and a reduction in proliferation which target the cranial neural crest cells as they start to migrate (27). We therefore analyzed apoptosis (TUNEL-positive cells) and proliferation (PCNA-positive cells) in the developing neural crest-derived auditory bulla at the initiation of the 'growth window'. Cell counting analysis of proliferating cells at P9 showed that proliferation was reduced during mutant auditory bulla formation in *Tcof1/DBA1*$^{+/-}$ mice (Fig. 7A–D; Table 5). In contrast, no change in the number of TUNEL-positive cells was observed (data not shown), indicating that the size defect was caused by reduced proliferation alone.

To rule out the possibility that the failure in mesenchymal clearance might be due to a reduction in apoptosis in the

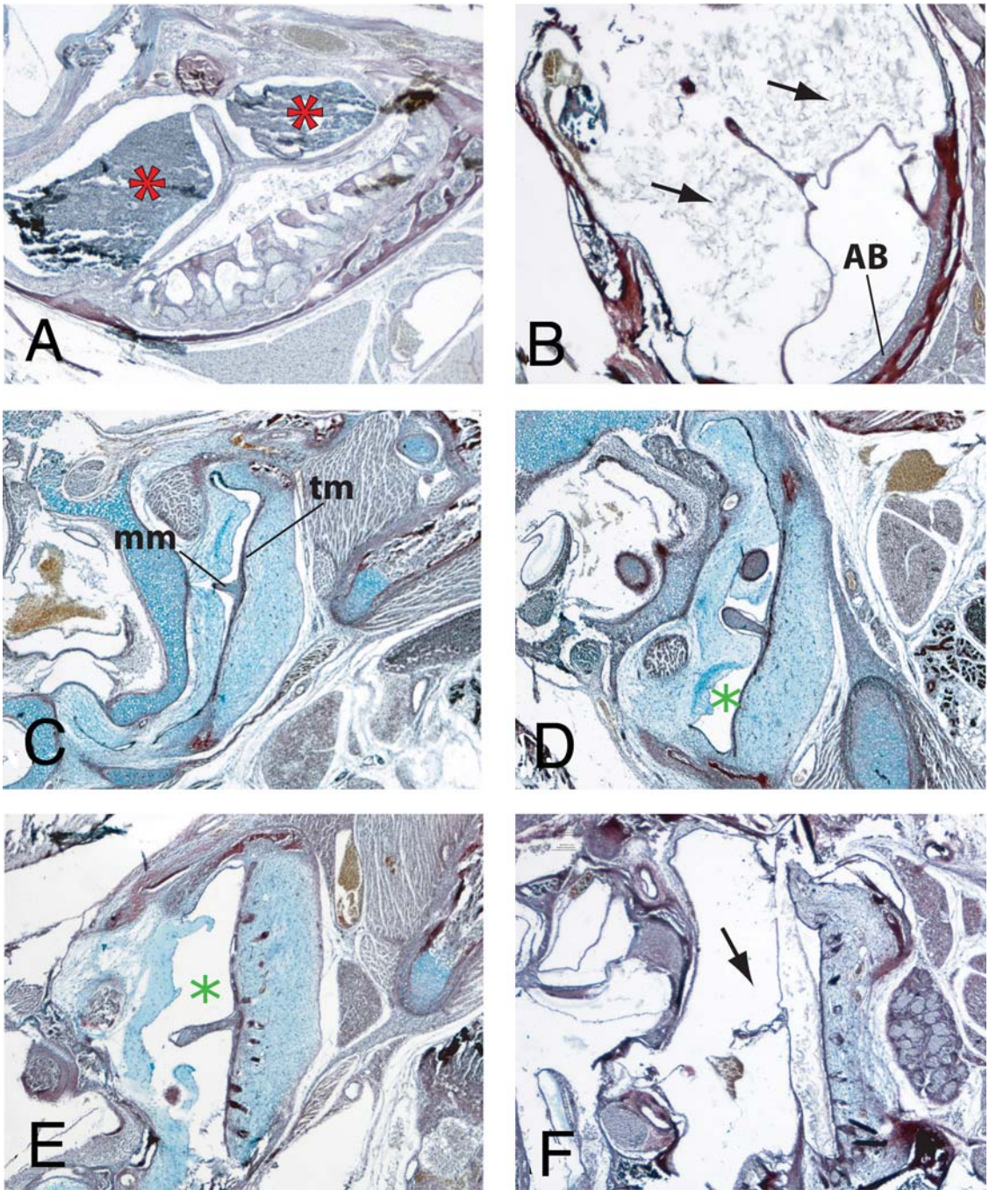

Figure 3. Histological analysis of cavitation. Syrius red-stained sections of ears in (**A**) *Tcof1*$^{+/-}$ and (**B**–**F**) wild-type mice. (A) At P14 the middle ears of *Tcof1*$^{+/-}$ mice are filled with mesenchyme (red asterisks) that surrounds the tympanic membrane and ossicles. (B) In P14 wild-type littermates, the middle ear space is free of mesenchyme and almost completely clear (arrows). Cavitation in wild-type mice at (C) P1; (D) P3; (E) P6; (F) P11. Green asterisks indicate middle ear mesenchyme. AB, auditory bulla ossified bone; mm, manubrium of malleus; tm, tympanic membrane.

Tcof1$^{+/-}$ mesenchyme, apoptosis was also investigated in the postnatal mesenchyme. Previously published TUNEL staining in the mouse middle ear showed the highest levels of apoptosis in the middle ear mesenchyme at P1, at the start of the cavitation process (13). In our studies, a few TUNEL-positive cells were observed in the WT middle ear mesenchyme throughout the period of cavitation, with sporadic positive cells observed at P1. A similar low level of positive cells was observed in the *Tcof1* mutant middle ears, indicating that loss of apoptosis was not the driving force behind the persistence of mesenchyme (Supplementary Material, Fig. S2).

DISCUSSION

Residual mesenchyme in the middle ear space has been linked to human disorders such as otitis media and cholesteatoma

Table 2. Mesenchyme correlation

Genotype	Preyer reflex	Mesenchyme present in right ear	Mesenchyme present in left ear	Mesenchyme present in both ears	No mesenchyme present	Total
Tcof1/DBA1$^{+/-}$	Positive	1	3	1	—	5
	Negative	—	—	14	—	14
WT	Positive	—	—	—	22	22
	Negative	—	—	—	—	0

The absence of a positive Preyer reflex response is linked to the presence of mesenchyme in both ears.

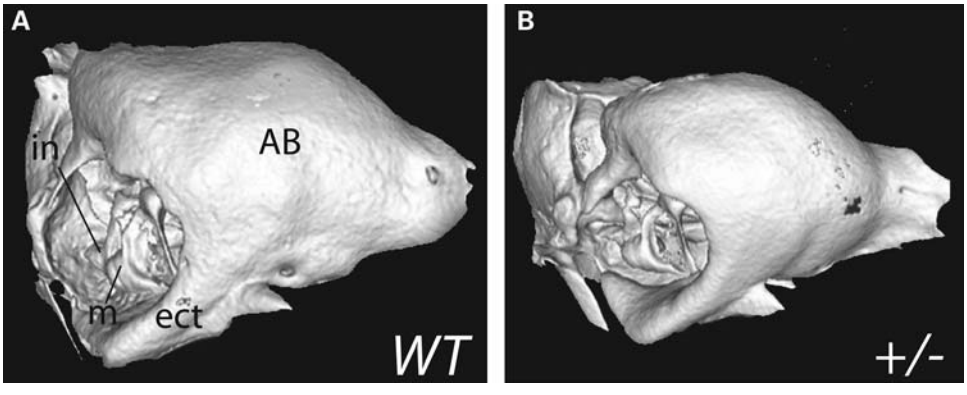

Figure 4. MicroCT reconstructions of adult auditory bullae. (**A**) Wild-type and (**B**) *Tcof1/DBA1*$^{+/-}$ mice. The mutant bulla appears significantly smaller than its wild-type littermate. AB, auditory bulla; ect, ectotympanic ring; I, incus; m, malleus.

Table 3. Mean volume of the middle ear cavity in *Tcof1/DBA1*$^{+/-}$ mice compared with their wild-type littermates in different age groups

Genotype	Volumetric analysis	Days after birth					
		6	9	12	15	21	Adult
WT	Mean volume (mm^3)	4.854	6.507	7.183	7.583	8.143	8.413
	SD	0.133	0.182	0.163	0.147	0.139	0.118
	n	5	5	3	4	12	4
Tcof1/DBA1$^{+/-}$	Mean volume (mm^3)	4.501	5.990	6.232	6.400	6.578	6.593
	SD	0.195	0.139	0.202	0.131	0.110	0.145
	n	3	4	3	6	12	4

Student's *t*-test at each developmental stage reveals a statistically significant decrease in mutant middle ear volume ($P < 0.001$).

(middle ear cyst), and is a contributing factor in incidences of CHL, the form of deafness diagnosed in ~50% of TCS patients. Most research to date has focused on establishing the molecular mechanisms underlying hearing loss associated with inner ear disruptions (32). An understanding of the contributions of the middle ear to deafness has been restricted predominantly to the development of the middle ear ossicles, with less understood about the formation of the middle ear space itself. It is known that the middle ear space is formed through cavitation, a predominantly postnatal process in mice. Clearance of the embryonic mesenchyme, in which the embedded middle ear ossicles initially develop, is required to ultimately generate an air-filled middle ear space across which sound vibrations can be transmitted. Failure to complete this process results in hearing loss. It is therefore of considerable interest that we have identified a loss-of-function mouse model for cavitation that has permitted a detailed analysis of the defect.

Our studies have revealed a previously unestablished link between middle ear cavitation and auditory bulla development (Fig. 8). The auditory bulla is the encompassing intramembranous bony capsule that surrounds the middle ear space. Using *Wnt1cre-lacZ* reporter mice, we have shown that the auditory bulla and middle ear mesenchyme are of neural crest origin, while the *pars cochlearis* around the inner ear is not of neural crest origin; these results are consistent with previous fate mapping studies using *Mespcre*/Rosa26 reporter mice (31). The observation that *Tcof1* expression is restricted to the neural crest cells of the early head, explains why the non-neural crest-derived inner ear is unaffected in our mouse model and in most patients with TCS (21,25). In *Tcof1/DBA1*$^{+/-}$ mice the auditory bulla is reduced in size and middle ear mesenchymal tissue persists into adult life. Hearing tests in animals with these defects revealed that hearing loss correlated directly with a smaller, mesenchyme-filled auditory bulla. Detailed staging of the development of the murine auditory bulla revealed that there is a critical 'growth window' during development of this structure. A recognizable bulla 'outline' is detectable by P6; however, the most notable growth occurs between P9 and P14. Although cavitation starts at prenatal stages, this auditory bulla growth period occurs during the time when the majority of mesenchyme disappears from the middle ear, so that by P14 the bulla has reached a maximal size, there is no mesenchymal tissue

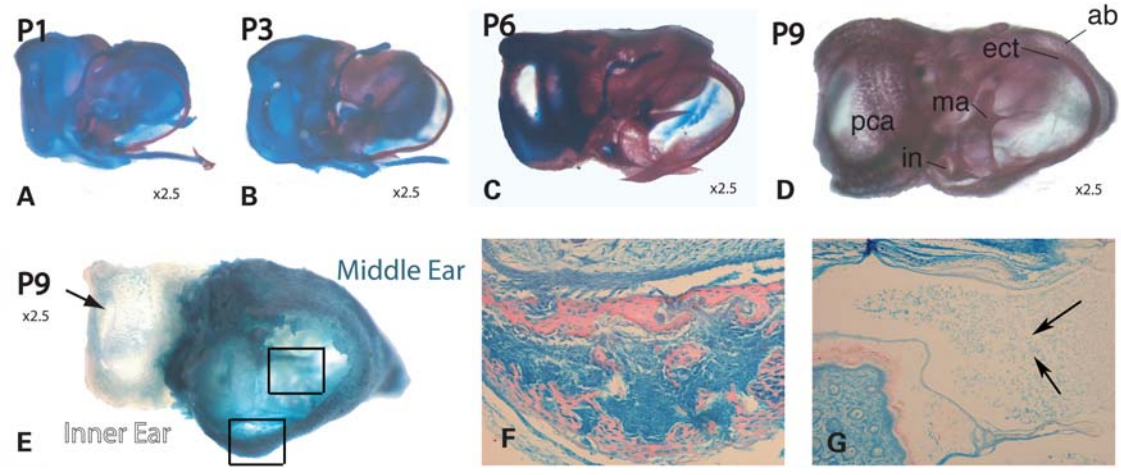

Figure 5. Intramembranous ossification of the auditory bulla in wild-type mice. Alizarin red and Alcian blue skeletal preparations of (**A**) P0, (**B**) P3, (**C**) P6, and (**D**) P9 bullae. The alizarin red stains the forming bone, while the alcian blue stains the cartilaginous structures. Final auditory bulla pattern is achieved by P9. (**E**) β-galactosidase staining of *Wnt1-Cre/Rosa26* middle ear structures at P9 reveals that the auditory bulla is neural crest-derived (blue staining). The cochlea (*pars cochlearis*), inner ear structure, is highlighted here (arrow) as an internal neural crest negative control (black arrow, unstained). (**F**) Section through lower black box in (E) showing the auditory bulla stained blue. The bone matrix stains pink with the Eosin counterstain. (**G**) Section through upper box in (E). The blue stained manubrium is at the top of the section with the outer ear at the lower left. The disappearing middle ear mesenchyme is of neural crest origin. The epithelium of the outer ear stains pick with Eosin. ab, auditory bulla; ect, ectotympanic ring; in, incus; ma, malleus; pca, *pars cochlearis* (cochlea).

Table 4. Correlation between middle ear volume and presence of mesenchyme

Mouse	Middle ear volume (mm^3)		Presence of mesenchyme	
	Right	Left	Right	Left
WT control	7.76	7.69	N	N
Tcof1/DBA1$^{+/-}$				
1.	6.42	6.95	Y	N
2.	8.05	6.53	N	Y
3.	6.39	5.76	N	Y
4.	6.95	6.64	N	N
5.	6.44	7.76	Y	N
6.	6.68	6.69	N	N
7.	5.82	6.65	Y	N
8.	5.66	5.94	Y	Y
9.	6.94	6.43	N	Y
10.	6.42	6.95	Y	N

10-week-old mice analysed via microCT. The presence of mesenchyme is correlated with a small size of bulla at a significance of $P = 0.0024$.

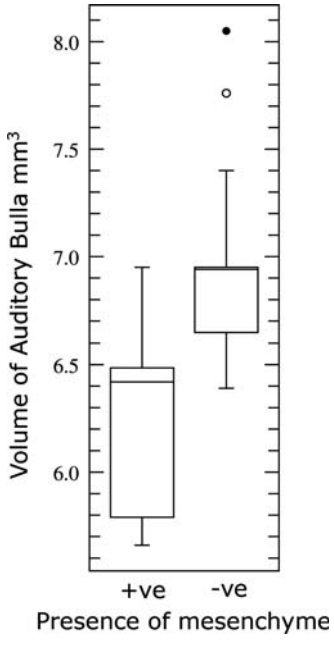

Figure 6. Data from Table 4 represented as a box plot to show size of auditory bulla in *Tcof1/DBA*$^{+/-}$ with and without retained mesenchyme.

remaining, and the animal can hear effectively. The process of bulla expansion and clearance of the middle ear appear linked, as within mutants, mesenchyme was only present in those ears where the bulla had failed to reach a certain size (around 6.5 mm^3; Table 4 and Figure 6). The failure of the bulla to expand, may in turn lead to a failure in the removal of mesenchyme. Alternatively retention of mesenchyme may prevent proliferation and expansion of the bulla, or these two processes may involve independent but interconnected mechanisms. These are important points and should be addressed in the future to enhance our understanding of middle ear development.

In *Tcof1/DBA1*$^{+/-}$ mice, while normal patterning occurs, there is a failure in proliferation of the auditory bulla. The defect in the size of the auditory bulla is likely to represent the culmination of a subtle reduction in the number of neural crest cells at much earlier stages of neural crest development. *Tcof1* expression has previously been shown to be down-regulated in the neural crest of the face at E12.5, and in keeping with this observation, no *Tcof1* expression was detected in postnatal heads in the current study (data not shown). In *Tcof1*$^{+/-}$ mice on a different genetic background on which the phenotype is more severe, a reduction in the ret-

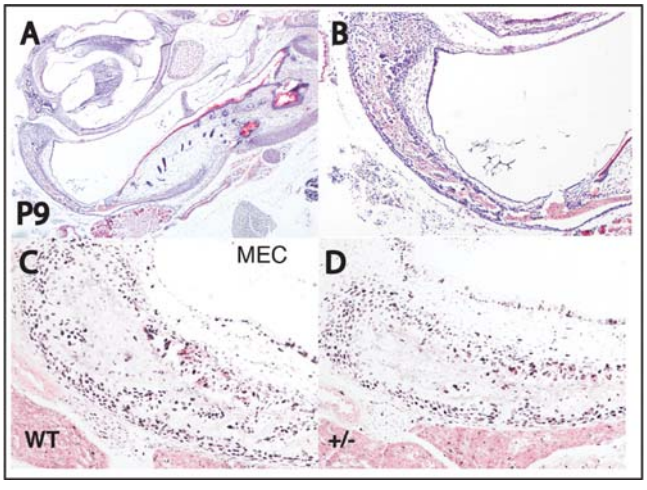

Figure 7. Reduced auditory bulla growth in *Tcof1/DBA1*$^{+/-}$ mice is associated with a reduction in proliferation in the developing intramembranous bone. (**A** and **B**) Ossifying auditory bulla in P9 wild-type mice as detected by haematoxylin and eosin staining. (B) Close-up of developing bone. (**C** and **D**) PCNA detection revealing cell proliferation (black cells). Reduced cell proliferation is detected in the mutant bulla (D) compared with a WT littermate (C), confirmed by Image J cell counting. MEC, middle ear cavity.

Table 5. Proliferation in the auditory bulla

Genotype	Auditory bulla—proliferating cells		Auditory bulla—total cell number	
	WT	*Tcof1/DBA1*$^{+/-}$	WT	*Tcof1/DBA1*$^{+/-}$
n	3	3	3	3
Mean	434.00	352.22	665.67	657.67
SD	2.65	23.63	9.45	2.52
P-value	0.0218[a]		0.19	

Tcof1/DBA1$^{+/-}$ sections of the auditory bulla at P9 compared with WT. Proliferating cells were identified by the presence of PCNA positive staining.
[a]There is a significant reduction in the number of proliferating cells in the auditory bulla of the mutant tissue compared with WT.

rotympanic process of the temporal bone was noted at E17.5, a key bone in the formation of the auditory bulla (27). Skeletal analysis of mice in which the *Tcof1* mutation resides on the DBA/1 background used in this study, indicated that there was no difference in the size of this element at P0; however, it is possible a slight reduction was missed. The phenotype may only become apparent after the auditory bulla has formed and starts to proliferate, with a slight depletion in cells becoming more pronounced as the bulla expands during postnatal development. The failure in growth of the auditory bulla is associated with a reduction in the number of proliferating cells in this structure at P9.

Interestingly, an asymmetric hearing loss was observed in 30% of the mutant mice. This corresponds well with the reported 50% of human TCS patients with asymmetrical hearing loss (21). The hearing loss was found on both the left and right sides, indicting no obvious developmental bias. The defect noted in mice in which the *Tcof1* mutation resides on the DBA/1 background thus confirms the etiology of TCS syndrome. Uniquely, however, this relatively isolated defect allows the analysis of a little understood process, middle ear cavitation. From our research to date it is clear that middle ear cavitation is a process linked closely to the development of the surrounding bony compartments, and that cavitation and problems therein can proceed independently of the development of the middle ear ossicles. As a next step in our understanding of middle ear cavitation defects, it is important to try and rescue the defects outlined above by stimulating proliferation during the critical window of auditory bulla growth and mesenchymal clearance. Small changes in proliferation might be able to have major effects on size of the bulla, and in turn may lead to a rescue of cavitation and hearing. Such experiments would have a major impact on treatment of patients with middle ear cavitation defects.

MATERIALS AND METHODS

Generation of mouse lines

Mice carrying a loss-of-function mutation in *Tcof1* on a DBA/1 genetic background were generated and genotyped as described previously (33). *Wnt-1Cre LacZ* reporter mice were generated as described previously (34). Timed-matings were set up such that noon of the day on which vaginal plugs were detected was considered embryonic day (E) 0.5. All animal procedures were reviewed, approved, and carried out under license issued by the Animals and Scientific Procedures Division of the Home Office, Her Majesty's Government, London, UK.

Histological and skeletal analysis

For histological analysis, dissected tissues were fixed in 4% paraformaldehyde at 4°C, decalcified in 10% EDTA in PBS for several weeks at 4°C, dehydrated through a series of ethanol washes, embedded in paraffin wax, sectioned as frontal or sagittal sections of 8–10 μm, and stained with syrius red or haematoxylin and eosin. For differential staining of bone and cartilage in whole-mount, tissues were processed as described previously (35).

Proliferation assay

Tissues were fixed in 4% PFA and embedded in paraffin wax. Sections were cut at 8–10 μm. A Zymed PCNA (proliferating cell nuclear antigen) staining reaction was performed according to the manufacturer's instructions (Invitrogen) with the following modifications: after rehydration, slides were treated for antigen-retrieval in 0.01 M citric acid pH 6.0 in a microwave oven for 10 min, followed by 0.05% Trypsin in PBS for 2 min, 0.1% Triton for 10 min and 50 mM NH_4Cl for 5 min. Products of the reaction were visualized with diaminobenzidine (DAB) and counterstained with eosin.

Preyer's reflex and ABR analyses

Hearing was initially assessed in mutant mice and their WT control siblings by ascertaining the presence or absence of pinna (Preyer's) reflex. The occurrence of a Preyer's reflex

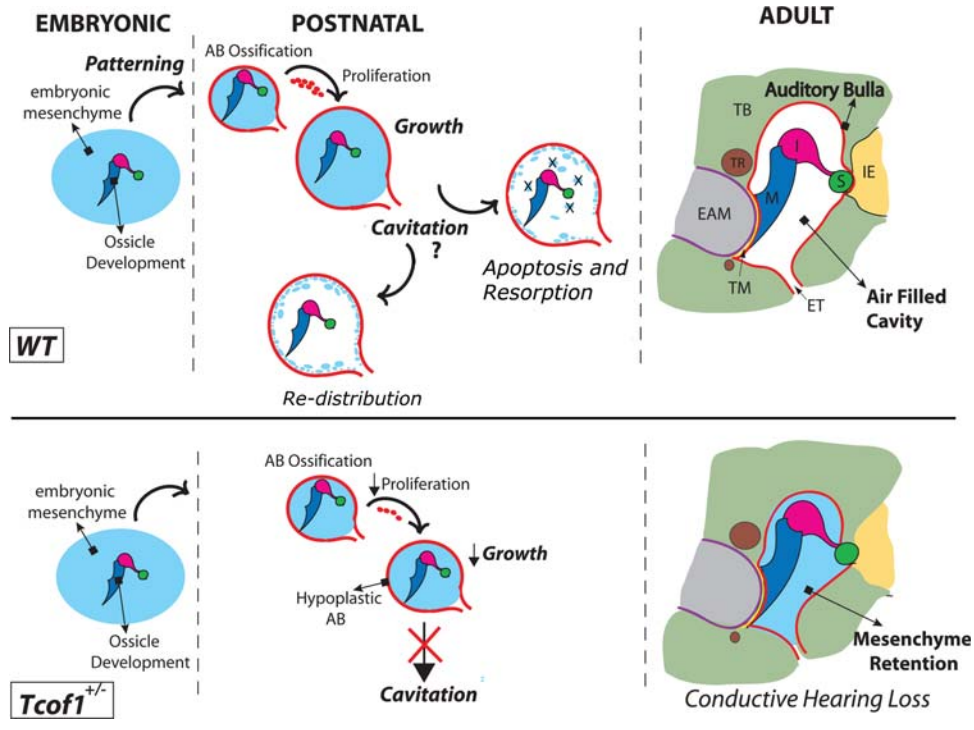

Figure 8. Middle ear cavitation is linked to growth of the auditory bulla (AB). Schematic of AB patterning and growth postnatally. Growth of the encompassing AB increases middle ear cavity volume. During the same time period the bulk of the mesenchyme is cleared from the middle ear. This may occur by a combination of apoptosis, resorption, and re-distribution. In the *Tcof1* mutant the growth of the auditory bulla is reduced and the mesenchyme fails to clear.

was determined in mice over 2 weeks of age by an observer who did not know their genotype. ABR measurements were performed to more accurately identify specific hearing thresholds. For ABR measurements, animals were anaesthetized with ketamine and medetomidine and placed within a large sound-attenuating chamber (Industrial Acoustics Company). Temperature was monitored using a temperature probe placed under the animal's abdomen, and maintained at 37.5 $\pm$ 0.5°C using a homeothermic blanket (Harvard Apparatus). The animal was positioned with the left ear oriented toward a free-field speaker (Tucker-Davis Technologies). Silver wire electrodes were threaded under the skin at the vertex (active electrode), ventrolateral to the left ear (reference electrode) and ventrolateral to the right ear (ground electrode). Click stimuli (50 ms duration, 20 clicks/s) were generated using a Tucker-Davis Technologies stimulus generation system (RX6, PA5, SA1, FF1) and calibrated to sound levels of 0–90 dB SPL based on the peak amplitude of the click as recorded using a Bruel & Kjaer 1/4′ microphone (Type 4134). Signals were acquired using a Tucker-Davis Technologies RA4LI low-impedance headstage connected to an RX5 Pentusa Base Station, bandpass filtered between 100 and 3000 Hz, amplified 1 000 000 times, recorded at an A/D sampling rate of 24 414 Hz, and analysed using custom MATLAB software (Mathworks). ABR thresholds were determined with 5 dB SPL precision based on visual inspection of evoked potentials averaged over 500–1000 click presentations at each sound level (presented in decreasing order), and were robust to small changes in body temperature ($\pm$ 0.5°C) or position of the ear ($\pm$ 0.5 cm).

MicroCT 3D reconstruction and volumetric analysis

Micro computerized tomography (microCT) was used for the three-dimensional description and volumetric analysis of mutant and wild-type auditory bullae.

Cell counting

ImageJ analysis software was utilized for cell counting purposes.

Statistics

Student's *t*-test was used to analyze the significance of the differences between mutant and wild-type auditory bulla tissues with respect to: the number of proliferating cells in PCNA-treated sections; microCT volumetric analysis at different stages of development. Student's *t*-test was also used to compare bulla volume in *Tcof1* mutant ears with and without mesenchyme.

TUNEL

Tissues were fixed in 4% PFA and embedded in paraffin wax. Sections were cut at 8–10 μm. Terminal deoxynucleotidyl transferase-mediated dUTP nick end labeling was used to detect apoptosis DNA breaks in individual cells (*In situ* Cell death detection kit; Chemicon). The procedure was carried out in accordance with manufacturer's instructions and con-

verted using a vectastain DAB substrate kit (Vectalabs). Eosin was used to counterstain the sections.

X-Gal staining

Staining with X-Gal was carried out by conventional methods (36) on dissected postnatal middle ears. Stained ears were wax embedded, sectioned and counterstained with Eosin.

SUPPLEMENTARY MATERIAL

Supplementary Material is available at *HMG* online.

ACKNOWLEDGEMENTS

Thanks to Chris Healy for the microCT scans of the auditory bullae. Thanks to Karen Liu and Yang Chai for use of the *Wnt1cre* reporter mice.

Conflict of Interest statement. None declared.

FUNDING

This work was supported by the Medical Research Council (MRC) [grant number G0501037].

REFERENCES

1. Baba, S., Ikezono, T., Pawankar, R. and Yagi, T. (2004) Congenital malformations of the middle ear with an intact external ear: a review of 38 cases. *ORL J. Otorhinolaryngol. Relat. Spec.*, **66**, 74–79.
2. Mallo, M. (2001) Formation of the middle ear: recent progress on the developmental and molecular mechanisms. *Dev. Biol.*, **231**, 410–419.
3. Mallo, M. (2003) Formation of the outer and middle ear, molecular mechanisms. *Curr. Top. Dev. Biol.*, **57**, 85–113.
4. Mallo, M. (1998) Embryological and genetic aspects of middle ear development. *Int. J. Dev. Biol.*, **42**, 11–22.
5. Mallo, M., Schrewe, H., Martin, J.F., Olson, E.N. and Ohnemus, S. (2000) Assembling a functional tympanic membrane: signals from the external acoustic meatus coordinate development of the malleal manubrium. *Development*, **127**, 4127–4136.
6. Hanken, J. and Hall, B.K. (1993) *The Skull: Patterns of Structural and Systematic Diversity.* University of Chicago Press, pp. 496–504.
7. Judkins, R.F. and Li, H. (1997) Surgical anatomy of the rat middle ear. *Otolaryngol. Head. Neck. Surg.*, **117**, 438–447.
8. Van der Klaauw, C.J. (1931) The auditory bulla in fossil animals. *Bull. Am. Museum Nat. Hist.*, **LXII**, 1–352.
9. Amin, S. and Tucker, A.S. (2006) Joint formation in the middle ear: lessons from the mouse and guinea pig. *Dev. Dyn.*, **235**, 1326–1333.
10. Jaskoll, T.F. and Maderson, P.F. (1978) A histological study of the development of the avian middle ear and tympanum. *Anat. Rec.*, **190**, 177–199.
11. Palva, T. and Ramsay, H. (2002) Fate of the mesenchyme in the process of pneumatization. *Otol. Neurotol.*, **23**, 192–199.
12. Palva, T., Paakko, P., Ramsay, H., Chrobok, V. and Simakova, E. (2003) Apoptosis and regression of embryonic mesenchyme in the development of the middle ear spaces. *Acta. Otolaryngol.*, **123**, 209–214.
13. Roberts, D.S. and Miller, S.A. (1998) Apoptosis in cavitation of middle ear space. *Anat. Rec.*, **251**, 286–289.
14. Nikolic, P., Jarlebank, L.E., Billett, T.E. and Thorne, P.R. (2000) Apoptosis in the developing rat cochlea and its related structures. *Dev. Brain Res.*, **119**, 75–83.
15. Piza, J.E., Northrop, C.C. and Eavey, R.D. (1996) Neonatal mesenchyme temporal bone study: typical receding pattern versus increase in Potter's sequence. *Laryngoscope*, **106**, 856–864.
16. Piza, J.E., Northrop, C.C. and Eavey, R.D. (1998) Embryonic middle ear mesenchyme disappears by redistribution. *Laryngoscope*, **108**, 1378–1381.
17. Jaisinghani, V.J., Paparella, M.M., Schachern, P.A., Schneider, D.S. and Le, C.T. (1999) Residual mesenchyme persisting into adulthood. *Am. J. Otolaryngol.*, **20**, 363–370.
18. Ruben, R.J. (2009) Serous otitis media in the 20th and 21st centuries: evolving views and treatments. *Acta. Otolaryngol.*, **129**, 343–347.
19. Takahara, T., Sando, I., Hashida, Y. and Shibahara, Y. (1986) Mesenchyme remaining in human temporal bones. *Otolaryngol. Head Neck Surg.*, **95**, 349–357.
20. Takahara, T. and Sando, I. (1987) Mesenchyme remaining in temporal bones from patients with congenital anomalies. A quantitative histopathologic study. *Ann. Otol. Rhinol. Laryngol.*, **96**, 333–339.
21. Pron, G., Galloway, C., Armstrong, D. and Posnick, J. (1993) Ear malformation and hearing loss in patients with Treacher Collins syndrome. *Cleft Palate Craniofac. J.*, **30**, 97–103.
22. Dixon, J., Trainor, P. and Dixon, M.J. (2007) Treacher Collins syndrome. *Orthod. Craniofac. Res.*, **10**, 88–95.
23. Hwang, C.H. and Wu, D.K. (2008) Noggin heterozygous mice: an animal model for congenital conductive hearing loss in humans. *Hum. Mol. Genet.*, **17**, 844–853.
24. Sakai, D. and Trainor, P.A. (2009) Treacher Collins syndrome: unmasking the role of Tcof1/treacle. *Int. J. Biochem. Cell Biol.*, **41**, 1229–1232.
25. Marszalek, B., Wojcicki, P., Kobus, K. and Trzeciak, W.H. (2002) Clinical features, treatment and genetic background of Treacher Collins syndrome. *J. Appl. Genet.*, **43**, 223–233.
26. Valdez, B.C., Henning, D., So, R.B., Dixon, J. and Dixon, M.J. (2004) The Treacher Collins syndrome (TCOF1) gene product is involved in ribosomal DNA gene transcription by interacting with upstream binding factor. *Proc. Natl Acad. Sci. USA*, **101**, 10709–10714.
27. Dixon, J., Jones, N.C., Sandell, L.L., Jayasinghe, S.M., Crane, J., Rey, J.P., Dixon, M.J. and Trainor, P.A. (2006) Tcof1/Treacle is required for neural crest cell formation and proliferation deficiencies that cause craniofacial abnormalities. *Proc. Natl. Acad. Sci. USA*, **103**, 13403–13408.
28. Dixon, J. and Dixon, M.J. (2004) Genetic background has a major effect on the penetrance and severity of craniofacial defects in mice heterozygous for the gene encoding the nucleolar protein Treacle. *Dev. Dyn.*, **229**, 907–914.
29. Jero, J., Coling, D.E. and Lalwani, A.K. (2001) The use of Preyer's reflex in evaluation of hearing in mice. *Acta. Otolaryngol.*, **121**, 585–589.
30. Huangfu, M. and Saunders, J.C. (1983) Auditory development in the mouse: structural maturation of the middle ear. *J. Morphol.*, **176**, 249–259.
31. McBratney-Owen, B., Iseki, S., Bamforth, S.D., Olsen, B.R. and Morriss-Kay, G.M. (2008) Development and tissue origins of the mammalian cranial base. *Dev. Biol.*, **322**, 121–132.
32. Vrijens, K., Van Laer, L. and Van Camp, G. (2008) Human hereditary hearing impairment: mouse models can help to solve the puzzle. *Hum. Genet.*, **124**, 325–348.
33. Dixon, J., Brakebusch, C., Fassler, R. and Dixon, M.J. (2000) Increased levels of apoptosis in the prefusion neural folds underlie the craniofacial disorder, Treacher Collins syndrome. *Hum. Mol. Genet.*, **9**, 1473–1480.
34. Chai, Y., Jiang, X., Ito, Y., Bringas, P. Jr, Han, J., Rowitch, D.H., Soriano, P., McMahon, A.P. and Sucov, H.M. (2000) Fate of the mammalian cranial neural crest during tooth and mandibular morphogenesis. *Development*, **127**, 1671–1679.
35. Depew, M.J. (2008) Analysis of skeletal ontogenesis through differential staining of bone and cartilage. *Methods Mol. Biol.*, **461**, 37–45.
36. Jiang, X., Iseki, S., Maxson, R., Sucov, H. and Morriss-Kay, G.M. (2002) Tissue origins and interactions in the mammalian skull vault. *Dev. Biol.*, **241**, 106–116.